Extraction of the surface waves and waveguide modes of the Green's function in layered anisotropic dielectrics between two ground planes

Ben Song and Wei Hong

State Key Laboratory of Millimeter Waves, Southeast University, Nanjing, People's Republic of China

Received 10 October 2000; revised 6 September 2001; accepted 5 October 2001; published 16 August 2002.

[1] In layered lossless dielectrics between two ground planes there exist the complicated waveguide modes as well as the surface waves in the electromagnetic field induced by a horizontal electric dipole. All these modes can be characterized by the rational parts with the real poles of the spectral domain vector and scalar potentials. The accurate extraction of these modes plays an important role in the evaluation of the Green's function in spatial domain. In our previous work [*Song and Hong*, 2002] a new algorithm based on rational approximation is presented for the extraction of surface waves and waveguide modes of the Green's function for layered isotropic dielectrics. In this paper, we extend the algorithm to the more complex case of layered anisotropic dielectrics; this algorithm can accurately extract all the real poles and their residues simultaneously. Thus we can get all the surface waves and waveguide modes, which can greatly help in the calculation of the spatial domain Green's function. The numerical results demonstrate the accuracy and efficiency of the proposed method. *INDEX TERMS:* 0644 Electromagnetics: Numerical methods; *KEYWORDS:* Green's function, surface waves, layered dielectrics, uniaxially anisotropic dielectrics, rational approximation

1. Introduction

[2] Because of its generality and rigorousness the incorporation of the spatial domain method of moments in the mixed-potential integral equation formulation has been one of the most popular methods for analyzing planar microwave integrated circuits [*Tsai et al.*, 1997; *Chang and Zheng*, 1992; *Mosig*, 1988]. With the planar circuits being more complicated, multilayer media are widely employed to make room for more versatile designs [*Tsai et al.*, 1997]. So, many efforts have been made to evaluate the Green's function of the multilayer medium [*Rahmat-Samii et al.*, 1981; *Kathei and Alexopoulos*, 1983; *Chow et al.*, 1991; *Yang et al.*, 1992; *Aksun*, 1996; *Hsieh and Kuo*, 1998], which is crucial for the success of the integral equation methods. All of these efforts fall into roughly two categories: the direct integration approaches and the complex image methods (CIM). The former numerically integrate the well-known Sommerfeld integral along either the real axis [*Kathei and Alexopoulos*, 1983] or a deformed path on the complex plane [*Rahmat-Samii et al.*, 1981]. When the integration is performed along the real axis, singularities of the integrand should be found out and removed in advance. As for the deformed path integration, the associated Bessel function with complex arguments may cause difficulty in obtaining accurate results. Recently, the fast Hankel transformation (FHT) algorithm has been proposed to accelerate the real-axis integration scheme for the calculation of the spatial domain Green's function [*Hsieh and Kuo*, 1998].

[3] By applying approximation techniques to the integrand, CIM can get the closed-form Green's function in the spatial domain finally via the Sommerfeld identity (SI) [*Chow et al.*, 1991; *Yang et al.*, 1992; *Aksun*, 1996]. With spectrum estimation techniques like the generalized pencil of function (GPOF) [*Sarkar and Pereira*, 1995], only a few closed-form complex images (images with complex amplitudes and locations) are needed to approximate the SI over a moderate distance range [*Aksun*, 1996]. The two-level scheme [*Aksun*, 1996] can make the choice of the numbers of complex images and sampling points and the endpoints of the sampling regions robust, which provides accurate representation of the Green's function and is much faster compared with the original one-level approximation.

[4] Microwave circuits are often enclosed in metal boxes to avoid radiation and coupling. The commonly used model for the analysis of the boxed circuits ignores the sidewalls; that is, only a layered structure

0048-6604/02/2000RS002572

between the two ground planes is considered. The features of the electromagnetic field by a horizontal electric dipole in such a structure have been studied [*Yang et al.*, 1992]. There exist not only the surface waves of both longitudinal section electric (LSE) and longitudinal section magnetic (LSM) types trapped by layered dielectrics but also the waveguide modes of both types trapped by the two ground planes. For the lossless cases all the propagating modes of these two kinds correspond to the rational parts with the real poles in the spectral domain. The only difference is as follows: All the poles of the propagating surface waves fall in the interval $[k_0, \varepsilon_{r,\max}k_0]$, while all the poles of propagating waveguide modes fall in $[0, k_0]$. Since both of them attenuate slowly, they dominate the far field together.

[5] The accurate extraction of surface waves and waveguide modes play an important role on the evaluation of the Green's function in the spatial domain. With these modes extracted analytically, the remainder of the spectral domain Green's function is smooth on the real axis. The smoothed integrand can facilitate the numerical integration along the real axis and is also ready for acceleration techniques such as FHT [*Hsieh and Kuo*, 1998]. The preextraction of the surface waves and waveguide modes is also helpful for CIM, because it can improve the approximation efficiency and provide a more precise characterization for the far field. A recent piece of research has even indicated that the extraction of surface waves is a prerequisite for the CIM when applied to the two-dimensional (2-D) cases [*Zhou et al.*, 1999].

[6] Because of the existence of the layered medium it is hard to accurately determine all the poles of the spectral domain Green's function on the real axis and their residues. Raising the operation frequency will make it even harder since the counts of poles will increase accordingly. To address the difficulty, a new extraction algorithm for the lossless layered isotropic medium was presented in our previous work [*Song and Hong*, 2002]. Different from the commonly used root-search-like algorithms, such as the bisection method, Muller's method, and Davidenko's method [*Muller*, 1956; *Johnson*, 1982; *Talisa*, 1985], there is no need to solve any transcendental equations, and all the real poles and their residues can be found out simultaneously with high accuracy and efficiency.

[7] In the practice of microwave circuit design and production, certain materials used as substrates exhibit dielectric anisotropy (occurring naturally or introduced during the manufacturing process). Furthermore, the anisotropy can also be used to improve the design [*Alexoplous and Krowne*, 1978]. So, in this paper, we will extend the algorithm to the more complex case of a layered uniaxially anisotropic/isotropic medium between the two ground planes. First, the spectral domain Green's function is formulated in terms of the Green's function of the cascading equivalent transmission lines model. Then a technique initialized for the simulation of transmission lines [*Celik and Cangellaris*, 1996] is applied to the model. Thus we can get the rational approximation of the spectral domain Green's function. The parts with real poles can be drawn and transformed into the spatial domain via Cauchy's residue theorem, and thus the propagating surface waves and waveguide modes of both LSE and LSM types are extracted.

[8] This paper is organized as follows: Section 2 presents the principle of the recommended algorithm. In section 3 some numerical examples are given for the validation of the method. In section 4 the conclusion is drawn. Some details about the presented method are described in Appendix A.

2. Principle

[9] Consider an infinitesimal horizontal electrical dipole of unit strength located on the interface between the mth and $(m + 1)$th dielectric layers of total N layers. The lossless dielectric layers are extended to infinity in both the x direction and the y direction. Each layer is assumed to be uniaxially anisotropic with relative permeability and permittivity as follows: $\underline{\underline{\mu}} = \underline{\underline{I}}_t\mu_t + \hat{z}\hat{z}\mu_z$, $\underline{\underline{\varepsilon}} = \underline{\underline{I}}_t\varepsilon_t + \hat{z}\hat{z}\,\varepsilon_z$, where $\underline{\underline{I}}_t$ is the transverse unit dyadic. Two perfect electric conductors (PECs) are placed at the top and bottom of this structure. The spectral domain Green's function for the vector $\tilde{G}_A$ and scalar $\tilde{G}_q$ potentials can be readily obtained from the spectral domain immittance method [*Michalski and Mosig*, 1997]. It can be described concisely as follows: First we can transfer the Maxwell equation into the spectral domain through the 2-D Fourier transformation and then split the equations according to the transverse and longitudinal field components. Revolving the coordinate system, we get the decoupled two sets of equivalent transmission lines, which corresponds to LSE (h) and LSM (e) modes, respectively. Therefore the stratified medium can be mapped into a cascading network of the equivalent transmission line segments of each layer, while a current source is made equivalent to the horizontal electrical dipole at the interface. Thus the spectral domain Green's function can be expressed as

$$\begin{cases} G_A(k_\rho) = \frac{\tilde{V}^h}{j\omega\mu_0}, \\ G_q(k_\rho) = -\frac{j\omega\varepsilon_0}{k_\rho^2}\left(\tilde{V}^h - \tilde{V}^e\right), \end{cases} \tag{1}$$

where $\tilde{V}^h$ and $\tilde{V}^e$ are the voltage response of the LSE mode and LSM mode transmission lines under the excitation of unit current source, respectively. According to equation (1) the spectral domain Green's function of

the stratified medium can be easily derived via the cascade of the equivalent transmission lines of each layer. The spectral domain Green's function of the layered medium between the two ground planes has three important features: (1) It has no branch point singularity since the multilayered structure is covered by two PECs; (2) all the poles lie on either the real axis or the imaginary axis; and (3) because $\widetilde{G}_{A,q}(k_\rho)$ is the even function of k_ρ, the poles appear as the pairs of $\pm k_{\rho,i}$. The spatial domain Green's function is the inverse Hankel transformation of $G_{A,q}(k_\rho)$.

$$G_{A,q}(\rho) = \frac{1}{4\pi}\int_{-\infty}^{+\infty} \widetilde{G}_{A,q}(k_\rho) H_0^{[2]}(k_\rho\rho) k_\rho dk_\rho. \quad (2)$$

It can be expressed as follows:

$$G_{A,q}(\rho) = G^e_{A,q}(\rho) + G^{\mathrm{SW}}_{A,q}(\rho), \quad (3)$$

where

$$G^e_{A,q}(\rho) = \frac{1}{4\pi}\int_{-\infty}^{+\infty} \widetilde{G}^e_{A,q}(k_\rho) H_0^{[2]}(k_\rho\rho) k_\rho dk_\rho, \quad (4)$$

$$\widetilde{G}^e_{A,q}(k_\rho) = \widetilde{G}_{A,q}(k_\rho) - \sum_m \frac{2k_{A,q,p_m}\mathrm{Res}_{A,q}(k_{A,q,p_m})}{k_\rho^2 - k^2_{A,q,p_m}}, \quad (5)$$

$$G^{\mathrm{SW}}_{A,q}(\rho) = \frac{1}{4\pi}(-2\pi j)\sum\nolimits_m \mathrm{Res}_{A,q}(k_{A,q,p_m}) \cdot H_0^{[2]}(k_{A,q,p_m}) k_{A,q,p_m}, \quad (6)$$

and $\mathrm{Res}_{A,q}(k_{A,q,p_m})$ represent the residues of $\widetilde{G}_{A,q}(k_\rho)$ at the real poles k_{A,q,p_m}. In equation (3), $G^{\mathrm{SW}}_{A,q}(\rho)$ is the potential for the propagating surface waves and the parallel-plate waveguide modes, which dominates equation (3) in the far-field region. From the modal expansion method the potential $G^e_{A,q}$ can be attributed to the contribution from the ρ-direction evanescent modes [*Yang et al.*, 1992]. From equation (1), $\widetilde{G}^{\mathrm{SW}}_{A,q}(k_\rho)$ can be determined by finding the real poles and the corresponding residues of the voltage response function of the equivalent transmission lines system, that is, $\widetilde{V}^h(k_\rho)$ and $\widetilde{V}^e(k_\rho)$. According to *Michalski and Mosig* [1997] the source-free Telegrapher's equations of the equivalent transmission lines of the *i*th layer are

$$\begin{cases} \frac{d\widetilde{V}^p_i}{dz} = -jk^p_{z,i} Z^p_i \widetilde{I}^p_i, \\ \frac{d\widetilde{I}^p_i}{dz} = -jk^p_{z,i} Y^p_i \widetilde{V}^p_i, \end{cases} \quad (7)$$

where superscript p means e or h, corresponding to LSM or LSE mode, respectively. The propagation constant, characteristic impedance, and admittance of the equivalent transmission lines are

$$\begin{cases} k^p_{z,i} = \sqrt{k^2_{t,i} - v^p_i k^2_\rho}, \\ Z^e_i = \frac{1}{Y^e_i} = \frac{k^e_{z,i}}{\omega\varepsilon_0\varepsilon_{t,i}}, \\ Z^h_i = \frac{1}{Y^h_i} = \frac{\omega\mu_0\mu_{t,i}}{k^h_{z,i}}, \end{cases} \quad (8)$$

where $k_{t,i} = k_0\sqrt{\mu_{t,i}\varepsilon_{t,i}}$, $k_0 = \omega\sqrt{\mu_0\varepsilon_0}$ is the wave number of the free space, and $v^e_i = \frac{\varepsilon_{t,i}}{\varepsilon_{z,i}}$ and $v^h_i = \frac{\mu_{t,i}}{\mu_{z,i}}$ are referred to as the electric and magnetic anisotropy ratios, respectively. As to h mode, equation (7) can be rewritten as follows by substituting equation (8) into it:

$$\begin{cases} \frac{dV^h_i}{dz} = -j\omega\mu_0\mu_{t,i} I^h_i, \\ \frac{dI^h_i}{dz} = \left(-\frac{j}{\omega\mu_0\mu_{t,i}} k^2_{t,i} + \frac{j}{\omega\mu_0\mu_{z,i}k^2_r}\right) V^h_i. \end{cases} \quad (9)$$

Let $s = k_\rho^2/k_0^2$, so

$$\begin{cases} \frac{dV^h_i(s,z)}{dz} = -\left(j\omega\mu_0\mu_{t,i}\right) I^h_i(s,z), \\ \frac{dI^h_i(s,z)}{dz} = -\left(j\omega\varepsilon_0\varepsilon_{t,i} - \frac{j\omega\varepsilon_0}{\mu_{z,i}}s\right) V^h_i(s,z). \end{cases} \quad (10)$$

or

$$\begin{cases} \frac{dV^h_i(s,z)}{dz} = -\left(R^h_i + sL^h_i\right) I^h_i(s,z), \\ \frac{dI^h_i(s,z)}{dz} = -\left(G^h_i + sC^h_i\right) V^h_i(s,z). \end{cases} \quad (11)$$

Here

$$R^h_i = j\omega\mu_0\mu_{t,i}, L^h_i \equiv 0, G^h_i = j\omega\varepsilon_0\varepsilon_{t,i}, C^h_i = -\frac{j\omega\varepsilon_0}{\mu_{z,i}}. \quad (12)$$

As to e mode, similarly, we have

$$\begin{cases} \frac{dV^e_i(s,z)}{dz} = -\left(R^e_i + sL^e_i\right) I^e_i(s,z), \\ \frac{dI^e_i(s,z)}{dz} = -\left(G^e_i + sC^e_i\right) V^e_i(s,z), \end{cases} \quad (13)$$

where

$$R^e_i = j\omega\mu_0\mu_{t,i} \bullet L^e_i = -\frac{j\omega\mu_0}{\varepsilon_{z,i}} \bullet G^e_i = j\omega\varepsilon_0\varepsilon_{t,i} \bullet C^e_i \equiv 0. \quad (14)$$

Now, both the equations of LSE and LSM modes, that is, equations (11) and (13), are in the form of the Telegrapher's equations in s domain (the Laplace transformation domain), where R^p_i, L^p_i, G^p_i and C^p_i are the equivalent unit-length parameters independent of variable s. Because the equivalent transmission line of each layer has the same variables s, the techniques initialized by *Celik and Cangellaris* [1996] can be adopted to acquire the rational approximation of the

voltage response $\tilde{V}^p(k_\rho)$. The procedure can be briefly described as follows: (1) Get the equivalent linear subnetwork of each transmission line segment via the order-M Chebyshev pseudospectral techniques. (2) Assemble all of the subnetwork into a whole equation to get the linear system of s. (3) Get the rational approximation of the voltage Green's function via the Krylov subspace technique based on the Arnoldi algorithm. More details about the above procedure can be found in Appendix A. Assume that the order-q rational approximation of the voltage response function is

$$\widetilde{V}^p(s) \doteq \widetilde{V}^p_{M,q}(s) = \sum_{n=1}^{q} \frac{\gamma_n^p}{s - \eta_n^p}. \tag{15}$$

Because $s = k_\rho^2/k_0^2$, equation (15) can be changed into

$$\widetilde{V}^p(k_\rho) = \sum_{n}^{N^p} \frac{2k_{\rho,p_n}\mathrm{Res}(k_{\rho,p_n})}{k_\rho^2 - k_{\rho,p_n}^2} + V^{p,e}(k_\rho). \tag{16}$$

Here, the first term of the right side stands for the rational parts related to the real-axis poles, k_{ρ,p_n} is the poles on the real-axis, and $Res(k_{\rho,p_n})$ are the corresponding residues; the second term of the right side corresponds to the rational parts of the rest of the poles. According to equation (16) and the upper part of equation (1)), $\tilde{G}_A^{SW}(k_\rho)$ is

$$\widetilde{G}_A^{\mathrm{SW}}(k_\rho) = \left(\frac{1}{j\omega\mu_0}\right) \cdot \sum_m \frac{2k_{h,\rho_m}\mathrm{Res}(k_{h,p_m})}{k_\rho^2 - k_{h,p_m}^2}. \tag{17}$$

As to the lower part of equation (1), because $k_\rho = 0$ is not the pole of $\tilde{G}_q(k_\rho)$, so we can get the right expression of the surface wave part of $\tilde{G}_q(k_\rho)$ after the modification of the residues

$$\widetilde{G}_q^{\mathrm{SW}}(k_\rho) = -j\omega\varepsilon_0 \left\{ \sum_m \frac{2\left[\mathrm{Res}(k_{h,p_m})/k_{h,p_m}\right]}{k_\rho^2 - k_{h,p_m}^2} - \sum_m \frac{2\left[\mathrm{Res}(k_{e,p_m})/k_{e,p_m}\right]}{k_\rho^2 - k_{e,p_m}^2} \right\}. \tag{18}$$

According to equations (6), (17), and (18) we can finally get $G_{A,q}^{SW}$ via the residue theorem

$$G_A^{\mathrm{SW}}(\rho) = \sum_m \mathrm{Res}(k_{h,p_m}) H_0^{[2]}(k_{h,p_m}\rho) k_{h,p_m}, \tag{19}$$

$$G_q^{\mathrm{SW}}(\rho) = \sum_m \frac{\mathrm{Res}(k_{h,p_m})}{k_{h,p_m}} H_0^{[2]}(k_{h,p_m}\rho) - \sum_m \frac{\mathrm{Res}(k_{e,p_m})}{k_{e,p_m}} H_0^{[2]}(k_{e,p_m}\rho). \tag{20}$$

Thus we have acquired all the propagating surface wave and waveguide modes.

[10] The parameters M and q determine the computation efficiency of the above method. After many numerical experiments we can give the following heuristic rules for the choice of M and q: (1) For each layer, M can be chosen identical; (2) $M > 10$; and (3) $q > \tilde{N}/4$. The meaning of $\tilde{N}$ can be found in Appendix A. According to Appendix A the above choice of M and q means rather high computation efficiency.

3. Numerical Results

3.1. A Structure of Three Isotropic Layers

[11] This structure is shown in Figure 1. From bottom to top the relative permittivity of each layer is 10.2, 2.2, and 1.0, and the thickness is 0.508 mm, 0.254 mm, and 9.238 mm. Both the source and the observation point are located on the interface between the second and the third layer. The operation frequency is 20 GHz. For the sake of simplicity, here we only consider the scalar potential Green's function $G_q(\rho)$. *Hsieh and Kuo* [1998] found three poles on the positive real axis. They are two poles of LSM mode ($k_{e,\rho_1}/k_0 = 0.7194$ and $k_{e,\rho_2}/k_0 = 1.055$) and one pole of LSE mode ($k_{e,\rho_1}/k_0 = 0.6708$). Hsieh and Kuo did not give the corresponding residues. We also found three real poles by using the recommended algorithm. They are two poles of LSM mode ($k_{e,\rho_1}/k_0 = 0.7198$ and $k_{e,\rho_2}/k_0 = 1.055$) and one pole of LSE mode ($k_{h,\rho_1}/k_0 = 0.6712$). The residues of these poles are determined simultaneously as -0.01901, -0.07225, and 0.05623. Because our results are somewhat different from the results of Hsieh and Kuo on the positions of two poles, we calculated the exact values of the spectral domain Green's function on these poles to show the accuracy of our algorithm. As shown in Table 1, the poles of our results approach more closely to singularity, which implies the accuracy of our algorithm. In order to check the accuracy of the resulting residues we can get the residues via the residue calculus. The relative errors between the residues resulting from the two methods are all less than 10^{-9}. After the extraction of all the propagating surface waves the spatial domain Green's function can be evaluated by the real-axis integration techniques. As shown in Figure 1, our results agree excellently with the results of Hsieh and Kuo up to the far field ($\rho = 10\lambda_0$).

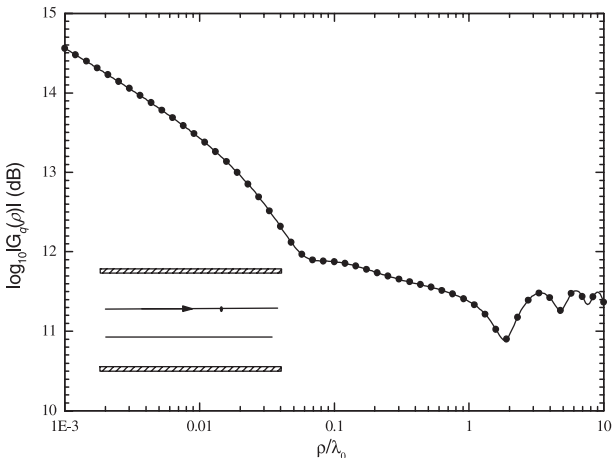

Figure 1. Logarithm of the magnitude of $G_q(\rho)$ induced by a dipole in a shield structure. Solid line, calculated by the combination of the presented surface wave extraction method and the real-axis integration method. Circles, results from *Hsieh and Kuo* [1998].

3.2. A Structure Containing Multianisotropic Layers

[12] Consider the four-layer structure shown in Figure 2. The two layers on the bottom are uniaxially anisotropic, and their relative permittivities are $\underline{\underline{\varepsilon}}_{r,1} = \underline{\underline{I}}_t 9.4 + \hat{z}\hat{z}11.6$ and $\underline{\underline{\varepsilon}}_{r,1} = \underline{\underline{I}}_t 9.4 + \hat{z}\hat{z}11.6$. The upper two layers are all isotropic, and their relative permittivities are $\varepsilon_{r,3} = 2.2$ and $\varepsilon_{r,4} = 1.0$, respectively. From bottom to top, the thickness of each layer is 1.0 mm, 0.5 mm, 0.35 mm, and 0.5 mm, respectively. The positions of the horizontal electric dipole and observation point are shown in Figure 2. The operation frequency is 30 GHz. We calculate the curve of $G_A(\rho)$ and $G_q(\rho)$ versus the source field range ρ via the following two methods: the numerical integration method without the extraction of surface wave and the numerical integration method combined with the presented surface wave extraction algorithm, respectively. The results are shown in Figures 3 and 4. Excellent agreement is observed here also.

Table 1. Magnitudes of the Spectral Green's Function on the Two Poles

k_ρ/k_0	$\lvert G_q(k_\rho)\rvert$	$\lvert G_A(k\rho)\rvert$
$k_{e,\rho_1}/k_0 = 0.7194$ [*Hsieh and Kuo*, 1998]	226.569	102.711
$k_{e,x_1}/k_0 = 0.7198$ (this paper)	1.895×10^{12}	8.535×10^{11}
$k_{h,x_1}/k_0 = 0.6708$ [*Hsieh and Kuo*, 1998]	266.149	
$k_{h,x_1}/k_0 = 0.6712$ (this paper)	5.793×10^{12}	

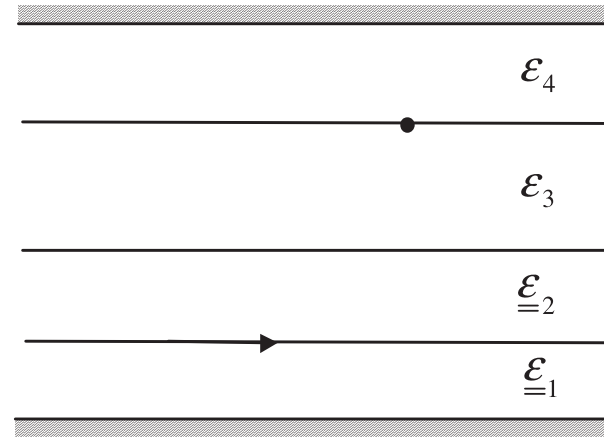

Figure 2. A four-layer structure containing two uniaxially anisotropic layers.

4. Conclusion

[13] In this paper, a new algorithm based on rational approximation is presented that can accurately extract all the real poles and the corresponding residues of the spectral domain Green's functions simultaneously. Thus we can get all the surface wave and waveguide modes for the layered uniaxially anisotropic medium, which can greatly help the calculation of the spatial domain Green's function. The numerical results demonstrate the accuracy and efficiency of the proposed method.

Appendix A

[14] Considering a uniform two-conductor transmission line system of length l, its s-domain Telegrapher's equations are given by

$$\frac{d}{dx'}V(x',s) = -(R+sL)I(x',s) \qquad x' \in [0,l], \quad \text{(A1)}$$

$$\frac{d}{dx'}I(x',s) = -(G+sC)V(x',s) \qquad x' \in [0,l], \quad \text{(A2)}$$

where R, L, G, and C are frequency-independent per-unit-length resistance, inductance, conductance, and capacitance, respectively. The general approach to including a segment of transmission line systems into a circuit simulator is to treat them as a linear network appropriate for stamping into the overall circuit matrix. We begin with the transformation $x = 2x'/l - 1$ to map the domain $[0,l]$ onto the domain $[-1,1]$, which is

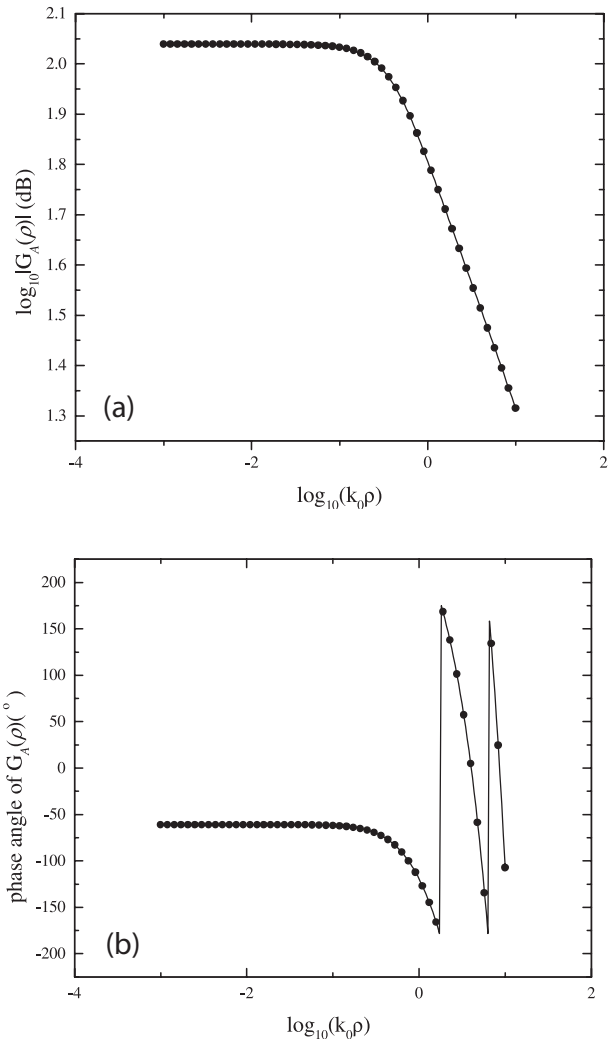

Figure 3. The $G_A(\rho)$ induced by a dipole in a shield structure: (a) the logarithm of the magnitude and (b) the phase angle. Solid line, calculated by the combination of the presented surface wave extraction method and the real-axis integration method. Circles, calculated by the real-axis integration method without surface wave extraction.

convenient for the later Chebyshev polynomial expansion. The transformed Telegrapher's equations are

$$\frac{d}{dx}V(x,s) = -\frac{l}{2}(R+sL)I(x,s) \qquad x \in [-1,1], \quad \text{(A3)}$$

$$\frac{d}{dx}I(x,s) = -\frac{l}{2}(G+sC)V(x,s) \qquad x \in [-1,1]. \quad \text{(A4)}$$

In the proposed methodology the line voltages and currents are approximated by their truncated Chebyshev expansions.

$$V(x,s) = \sum_{m=0}^{M} a_m(s)T_m(x), \quad \text{(A5)}$$

$$I(x,s) = \sum_{m=0}^{M} b_m(s)T_m(x), \quad \text{(A6)}$$

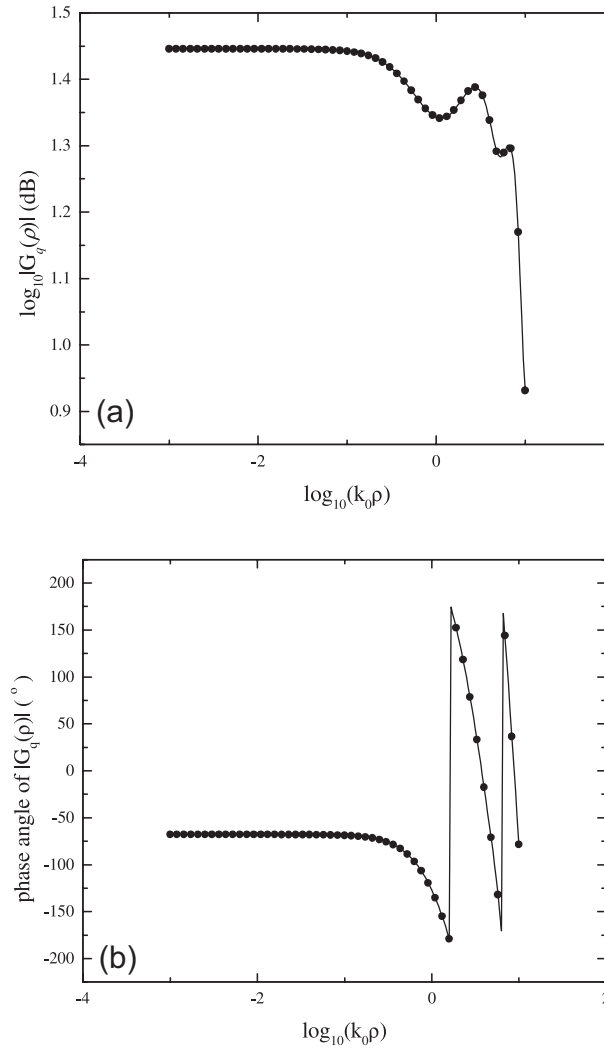

Figure 4. The $G_q(\rho)$ induced by a dipole in a shield structure: (a) the logarithm of the magnitude and (b) the phase angle. Solid line, calculated by the combination of the presented surface-wave extraction method and the real-axis integration method. Circles, calculated by the real-axis integration method without surface wave extraction.

where $T_m(x) = \cos(m\cos^{-1} x)$ is the mth-degree Chebyshev polynomial of the first type. Through the so-called pseudospectral approximation [*Celik and Cangellaris*, 1996] one can obtain

$$V(x,s) = \sum_{m=0}^{M} V(x_m,s) g_m(x), \tag{A7}$$

$$I(x,s) = \sum_{m=0}^{M} I(x_m,s) g_m(x), \tag{A8}$$

where $V(x_m,s)$ and $I(x_m,s)$ are the voltage and current at the points x_m defined by

$$x_m = \cos\frac{m\pi}{M} \qquad m = 0, 1, \ldots, M. \tag{A9}$$

So $x_0 = 1$ and $x_M = -1$ correspond to the far- and near-end terminals of the transmission line, respectively. In equations (A7) and (A8), $g_m(x)$ is a function with Lagrange-polynomial-type property

$$g_m(x) = \frac{(1-x^2)T'_M(x)(-1)^{m+1}}{c_m M^2 (x - x_m)}, \tag{A10}$$

where

$$c_m = \begin{cases} 1 & m \neq 0, M \\ 2 & \text{otherwise} \end{cases}, \qquad g_m(x_n) = \delta_{mn}.$$

To obtain a discrete approximation to the differential equations given in equations (A3) and (A4), a collocation method is used with collocation points in equation (A9). Thus the resultant system of equations in matrix form is

$$D\overline{V}_s(s) = -Z(s)\overline{I}_s(s), \tag{A11}$$

$$D\overline{I}_s(s) = -Y(s)\overline{V}_s(s), \tag{A12}$$

where

$$D = (D_{nm}) \in R^{(M+1)\times(M+1)}, \quad D_{nm} = \frac{d}{dx} g_m(x)|_{x=x_n}, \tag{A13}$$

$$Z(s) = \frac{l}{2}(R + sL)\cdot\bar{\bar{I}}, \qquad Y(s) = \frac{l}{2}(G + sC)\cdot\bar{\bar{I}}, \tag{A14}$$

$$\overline{V}_s(s) = [V(x_0,s), V(x_1,s), \ldots, V(x_M,s)]^T,$$
$$\overline{I}_s(s) = [I(x_0,s), I(x_1,s), \ldots, I(x_M,s)]^T.$$

Consider a cascading model containing total N transmission line segments. According to equations (A11) and (A12) there will be total of $2N(M + 1)$ equations and $2N(M + 1)$ variables. In fact, because of the existence of the interfaces and the short-circuit conditions in the terminals there are only $(N - 1)$ independent node voltages (the voltages at the interfaces). Besides, the current continuous condition can contribute another $(N - 1)$ equations. So the redundant equations and variables in the original matrix equations (A11) and (A12) for each line are cancelled, and the new formulation of each line can be simply written as

$$\left(A^R + sA^I\right)\overline{V}_t(s) + \left(B^R + sB^I\right)\overline{J}(s) = 0, \tag{A15}$$

where $\overline{V}_t(s)$ is the terminal voltage vector of the line and $\overline{J}(s)$ is the vector containing the terminal currents as well as the internal voltages and currents. Applying the Kirchhoff's current law to the (N − 1) interfaces and combining with the matrix equations of each line, we can establish the nodal analysis matrix equation of the whole circuit as

$$(G + sC)\overline{x} = \overline{b}, \tag{A16}$$

where G and C are all square real matrices with dimension of $\tilde{N}$ and $\overline{b}$ is a vector with all but one entry being zero. Here, $\tilde{N} = 2NM + N - 1$. Now, the model has been represented by a first-order system of s, and therefore the Krylov subspace order-reduction techniques can be applied. Let $V(s)$ be the output voltage of interest, say

$$V(s) = \overline{d}^T\overline{x}(s). \tag{A17}$$

Then, using equation (A16), the output frequency response is given by

$$V(s) = \overline{d}^T(G + sC)^{-1}\overline{b}. \tag{A18}$$

Using the change of $s = s_0 + \sigma$ and setting

$$A = -(G + s_0C)^{-1}C, \qquad \overline{r} = (G + s_0C)^{-1}\overline{b}, \tag{A19}$$

we can rewrite equation (A19) as follows:

$$V(s) = \overline{d}^T\left(\bar{\bar{I}} - \sigma A\right)^{-1}\overline{r}. \tag{A20}$$

A Krylov subspace order-reduction technique such as the Arnoldi-based algorithm can be applied to equation (A20) to acquire an efficient rational approximation for $V(s)$ steadily [*Silveria et al.*, 1996]. The resulting approximation of $V(s)$ can be expressed as

$$V(s_0 + \sigma) = \sum_{j=1}^{q} \frac{k_j}{\sigma - \lambda_j}. \tag{A21}$$

In this procedure the computational cost of the frequent matrix-vector product can be reduced by only one LU factorization of $(G + s_0C)$ and $2q$ forward-backward substitutions. Thus the dominant cost of the Pade via Lanczos algorithm is in computing the LU factorization of $(G + s_0C)$.

References

Aksun, M. I., A robust approach for the derivation of closed-form Green's functions, *IEEE Trans. Microwave Theory Tech.*, *44*, 651–658, 1996.

Alexoplous, N. G., and C. M. Krowne, Characteristics of single and coupled microstrip on anisotropic substrate, *IEEE Trans. Microwave Theory Tech.*, *26*, 387–392, 1978.

Celik, M., and A.C. Cangellaris, Simulation of dispersive multiconductor transmission lines by Padé approximation via the Lanczos process, *IEEE Trans. Microwave Theory Tech.*, *44*, 2525–2535, 1996.

Chang, D. C., and J. X. Zheng, Electromagnetic modeling of passive circuit elements in MMIC, *IEEE Trans. Microwave Theory Tech.*, *40*, 1741–1747, 1992.

Chow, Y. L., J. J. Yang, D. G. Fang, and G. E. Howard, A closed-form spatial Green's function for the thick microstrip substrate, *IEEE Trans. Microwave Theory Tech.*, *39*, 588–592, 1991.

Hsieh, R. C., and J. T. Kuo, Fast full-wave analysis of planar microstrip circuit elements in stratified media, *IEEE Trans. Microwave Theory Tech.*, *46*, 1291–1297, 1998.

Johnson, R. L., *Numerical Methods: A Software Approach*, John Wiley, New York, 1982.

Kathei, P. B., and N. G. Alexopoulos, Real axis integration of Sommerfeld integrals with applications to printed circuit antennas, *J. Math. Phys.*, *24*, 527–533, 1983.

Michalski, K. A., and J. R. Mosig, Multilayered media Green's functions in integral equation formulations, *IEEE Trans. Antennas Propag.*, *45*, 508–517, 1997.

Mosig, J. R., Arbitrarily shaped microstrip structures and their analysis with a mixed potential integral equation, *IEEE Trans. Microwave Theory Tech.*, *36*, 314–323, 1988.

Muller, D. E., A method for solving algebraic equations using automatic computer, *Math. Tables Aids Comput.*, *10*, 208–215, 1956.

Rahmat-Samii, Y., R. Mittra, and P. Parhami, Evaluation if Sommerfeld integrals for lossy half-space problems, *Electromagnetics*, *1*, 1–28, 1981.

Sarkar, T. K., and O. Pereira, Using the matrix pencil method to estimate the parameters of a sum of complex exponentials, *IEEE Antennas Propag. Mag.*, *37*(2), 48–55, 1995.

Silveria, L. M., M. Kamon, and J. White, Efficient reduced-order modeling of frequency dependent coupling inductances associated with 3-D interconnect structures, IEEE Trans. Components Packag, *Manuf. Technol., Part B: Adv. Packag.*, *19*(2), 283–288, 1996.

Song, B., and W. Hong, A new algorithm for the extraction of the surface waves for the Green's function in layered dielectrics, *Sci. China, Ser. F*, *45*(2), 143–151, 2002.

Talisa, S. H., Application of Davidenko's method to the solution of dispersion relations in lossy waveguide systems, *IEEE Trans. Microwave Theory Tech.*, *33*, 967–971, 1985.

Tsai, M. J., F. D. Flaviis, O. Fordham, and N. G. Alexopoulos, Modeling planar arbitrarily shaped microstrip elements in multilayered media, *IEEE Trans. Microwave Theory Tech.*, *45*, 330–337, 1997.

Yang, J. J., Y. L. Chow, G. E. Howard, and D. G. Fang, Complex images of an electric dipole in homogeneous and layered dielectrics between two ground planes, *IEEE Trans. Microwave Theory Tech.*, *40*, 595–600, 1992.

Zhou, G. R., N. N. Feng, and D. G. Feng, Application of full wave discrete image method in two-dimensional CPW structure, paper presented at International Conference on Computational Electromagnetics and Its Application (ICCEA'99), Inst. of Electr. and Electon. Eng., Beijing, 1999.

W. Hong and B. Song, State Key Laboratory of Millimeter Waves, Southeast University, Nanjing 210096, P. R. China. (weihong@seu.edu.cn)